Arabian Journal of Chemistry 16 (2023) 105306

Contents lists available at ScienceDirect

Arabian Journal of Chemistry

journal homepage: www.sciencedirect.com

Original article

# Synthesis, spectroscopic characterization, antileishmanial, DNA binding, antioxidant, cytotoxicity, antifungal and antibacterial studies of organotin(IV) carboxylate complexes

Shah Hussain [a], Shaukat Shujah [a,*], Abdul Rehman [b], Syed Tasleem Hussain [a], Mubbashir Hussain [b], Iffat Naz [c], Aiyeshah Alhodaib [d,*]

[a] Department of Chemistry, Kohat University of Science and Technology (KUST), Kohat 26000, Pakistan
[b] Department of Microbiology, Kohat University of Science and Technology (KUST), Kohat 26000, Pakistan
[c] Department of Biology, Deanship of Educational Services, Qassim University, Buraidah 51452, Saudi Arabia
[d] Department of Physics, College of Science, Qassim University, Buraidah 51452, Saudi Arabia

ARTICLE INFO

*Article history:*
Received 20 June 2023
Accepted 21 September 2023
Available online 26 September 2023

*Keywords:*
Orgnaonotin(IV)
Carboxylates
*Leishmaniatropica*
Antioxidant
SS-DNA

ABSTRACT

Six new organotin(IV) complexes, [$Bu_2SnL$] (**1**), [$Me_2SnL$] (**2**), [$Me_3SnL$] (**3**), [$Bu_3SnL$] (**4**), [$Ph_3SnL$] (**5**) and [($n$-$Oct_2SnL$] (**6**) have been synthesized from the reaction of 4-((5-chloro-2-hydroxyphenyl)ethylidenea mino)methyl)cyclohexanecarboxylic acid (HL) with the corresponding diorganotin(IV) dichloride/oxide or triorganotin(IV) chloride.All the synthesized compounds were structurally characterized by elemental analysis, FT-IR, multinuclear NMR ($^1$H and $^{13}$C) spectroscopies and powder X-ray diffraction analysis. The results of spectroscopic studies support coordination of oxygen donor site of the ligand with the tin atom of di andtriorgnaotin(IV) moieties. Currently, a vaccine for leishmaniasis remains unavailable, and the existing antimonial-based drugs are accompanied by significant and adverse side effects. The synthesized compounds were screened for antileishmanial activity against promastigotes form of *leishmania tropica*. Highest activity was shown by compound 2 with an $IC_{50}$ value of 1.17 ± 0.01 μg/mL, as compared to amphotericin B with $IC_{50}$ value of 0.71 ± 0.01 μg/mL The synthesized compounds were also subjected to interaction studies with single-stranded DNA (SS-DNA). Among these compounds, Compound **2** demonstrated the most substantial binding affinity, exhibiting a binding constant of $2.7x10^3$ $M^{-1}$. Furthermore, the compounds also showed excellent antioxidant potential with percentage radical scavenging value in the range of 87–95% and $IC_{50}$ 46.92, 72.10, 46.33 Mg/mL for compounds **1, 5** and **6**respectively. The complexes revealed significant toxicity with comparable $LD_{50}$(6.26 μg/mL), (6.79 μg/mL), (5.67 μg/mL)and (5.80 μg/mL)for complex **2, 3,5** and standard drug respectively. Similarly, the complexes also showed significance antifungal and antibacterial activity.



## 1. Introduction

Leishmaniasis is a vector born poverty associated disease caused by a grouped of parasites protozoan *leishmania*. The parasites are transmitted through female sand fly insect phlebotomy. More than twenty different *leishmaia* species infect humans. The parasites are transmitted through the bit of more than 90 sand fly species (Zafar et al., 2021). According to World Health Organization report about 1.3 million leishmaniasis cases registers and causing about 20,000 to 30,000 deaths annually (mondiale de la Santé & Organization, 2016). Leishmaniasis is a complex disease having two main epidemiological forms. Skin or cutaneous leishmaniasis is common type and characterized by skin sores. One million cases of cutaneous leishmaniasis have been registered

* Corresponding authors at: Department of Physics, College of Science, Qassim University, Buraidah 51452, Saudi Arabia(A. Alhodaib), Department of Chemistry, Kohat University of Science and Technology (KUST), Kohat, 26000, Pakistan(S. Shujah).
*E-mail addresses:* dr.shaukat@kust.edu.pk, shaukat.shujah@yahoo.com (S. Shujah), ahdieb@qu.edu.sa (A. Alhodaib).

Peer review under responsibility of King Saud University.

Production and hosting by Elsevier

https://doi.org/10.1016/j.arabjc.2023.105306
1878-5352/

annually in the last decades. Visceral leishmaniasis also known as kalaazar is more fatal and decisive than skin leishmaniasis and has worsen due to less understanding of the illness pathogenesis (Gradoni, 2018). The infection can developed in days or even in years after the bite of infected sand fly (Lipoldová & Demant, 2006). In visceral leishmaniasis internal organs including spleen, bone marrow and liver are commonly infected (Goto & Lindoso, 2004). WHO has reported that leishmaniasis is among the most fatal illness that requires to be treated and indicated foremost global health problem which gives a mild to wide spectrum of clinical appearances with severely lethal outputs (Kumar, Pandey, & Samant, 2020).

Unfortunately, no vaccine is available for the prevention and treatment of leishmaniasis. Therefore, medicines are the only available source for treatment of this illness (Mohammed et al., 2020). The available antileishmanial medicines are mainly based on antimonial treatment and lately urbanized and the tested medicament have shown a number of severe side effects. The pentavalent antimony based drugs such as sodium stibogluconate and meglumine antimonate are the primary option for leishmaniasis treatment(Maltezou, 2008). Although, these medicines are clinically utilized for a few decades, but the mechanism of action is still remain unclear(Tiwari et al., 2019). Moreover, other medicines like amphotericin B and pentamidine have also been employed but to severe side effect and high cost, the prescription of these drugs has been restricted. Subsequently, there has been a dire need for the development and discovery of new chemotherapeutics agent with none or less side effect for the prevention and ailment of leishmaniasis (Olías-Molero, de la Fuente, Cuquerella, Torrado, & Alunda, 2021).

Furthermore the chemotherapeutic drugs promote oxidative stress and raise the concentration of oxygen reactive species (ROS) which causes a number of health pathologies (Prieto-Bermejo, Romo-González, Pérez-Fernández, Ijurko, & Hernández-Hernández, 2018). Interestingly, when ROS molecules are generated in excess concentration, it has been reported to produce oxidative damage to DNA, proteins, lipids and various cell membranes (Prieto-Bermejo et al., 2018).

Deoxyribonucleic acid (DNA) is the most important bio macromolecule, as it plays key role in process of copying, storing, transmitting genes messages and guide the biochemical synthesis of enzymes and proteins through the process of transcription and replication of genetic information (Chen, Zhao, & He, 2016). DNA is also the major target for drugs and understanding the molecular mechanism of drugs action. The drugs molecules can interact with DNA via intercalation between DNA base pairs, groove binding or electrostatic binding to the sugar phosphate of DNA molecule (Alotaibi & Momen, 2019). DNA interaction investigation of organotin(IV) carboxylates has gotten remarkable interest during the recent years due to biomolecular compatibility. The organotin(IV) complexes recognizes specific DNA sequence, alter DNA structure, inhibit access to the repressor or activator proteins and finally the gene expression process (Tariq et al., 2021). Furthermore, organotin(IV) carboxylates attain unique stereo electronic configuration which underline their importance in the field of medicinal chemistry. A number of organotin(IV) carboxylates have been reported with significant antipathogenic activities which are greatly determined by the stereochemistry of organotin(IV) and oxidation number of tin atom. Consequently, organotin(IV) carboxylates have been a dynamic research area due to their attention grabbing structural motifs, varying from monomeric structure to supramolecular arrangement and biological potential which has drawn the interest of researchers toward their anti-leishmaniasis activity (Abbas, Ali, Hussain, & Shahzadi, 2013; Hadi, Jawad, Ahmed, & Yousif, 2019).

By considering all the information about organotin(IV) carboxylates we have reported a new series of six organotin(IV) carboxylates. The characterization of all prepared compounds was done by elemental analysis, FT-IR spectroscopy, NMR ($^1$H, $^{13}$C) spectroscopy and powder XRD. The synthesized compounds were investigated for antileishmanial activity, DNA interaction and antioxidant activity.

## 2. Materials and methods

### 2.1. Reagents and chemicals

All the reagents including4-(aminomethyl)cyclohexancarboxyli cacid,dimethyltin(IV) dichloride, dibutyltin(IV) dichloride, trimethyltin(IV) chloride, triphenyltin(IV) chloride and dioctyltin (IV) oxide were procured from Sigma-Aldrich (USA) and used as received. The solvents were purchased from Merck (Germany) and dried before use according to the standard procedure (D. B. G. Williams & Lawton, 2010) (Nadeem Muhammad et al., 2021). Sodium salt of Salmon sperm DNA was obtained from Acros. The electrothermal melting point apparatus Gallen Kamp was used for melting point determination. Elemental analysis was carried out using CE-440 Elemental Analyzer. Electronic spectra were recorded on a Shimadzu 1800 UV–visible spectrophotometer. FT-IR spectra were recorded on a Thermo Nicolet-6700 FT-IR in the scanning range of 4000–400 $cm^{-1}$ using KBr pellets. $^1$H and $^{13}$C NMR were recorded on a 400 MHz JEOL ECS instrument using deuterated chloroform and DMSO as solvent. The chemical shift values are given in ppm and coupling constant (*J*) values are provided in Hz. The $^1$HNMR signals multiplicity are given with chemical shift; (s = singlet, d = doublet, t = triplet, q = quartet, m = multiplet, dd = doublet of doublet). XRD pattern was recorded on an Oxford Diffraction Gemini diffractometer.

### 2.2. Synthesis

#### 2.2.1. Synthesis of ligand (NaL)

4-(aminomethyl)cyclohexanecarboxylic acid (0.5 g, 3.18 mmol) was suspended in 15 mL methanol in two necks round bottom flask fitted with a condenser. A clear solution was obtained after being stirred for 15 min. Equimolar solution of 5-chloro-2-hydroxyacetophenone (0.54 g, 3.18 mmol) was added to the reaction system. The general reaction is shown in Scheme 1. The reaction mixture was refluxed for 6 h. To this solution sodium bicarbonate (0.26 g, 3.18 mmol) was added and refluxed for 1 h. A bright yellow compound was obtained after evaporating the solvent at room temperature.

Yield 76%, m.p 174–176 °C; anal. (calc.) for $C_{16}H_{19}ClNNaO_3$: C, 56.13 (57.92); H, 5.11 (5.77); N, 3.96 (4.22);IR ($cm^{-1}$): 1686 υ $(COO)_{asym}$, 1438 υ$(COO)_{sym}$, 1586 υ(C = N), 3535 υ(OH); $^1$H NMR ($CDCl_3$-d) δ (ppm):12.14 (s, 1H, OH), 7.22 (d, *J* = 8.8 Hz,1H, phenyl), 7.45 (s, 1H, phenyl), 7.18 (d, *J* = 8.9 Hz, 1H, phenyl), 3.39 (d, *J* = 2.5 Hz, 2H, N-$CH_2$), 2.62 (s, 3H, $CH_3$),2.10 (p, *J* = 6.4 Hz, 1H, cyclohexyl), 1.91–1.93 (m, 2H, cyclohexyl), 1.48–1.51 (m, 2H, cyclohexyl), 1.11–1.26 (m,1H, cyclohexyl). $^{13}$C NMR ($CDCl_3$-d), δ (ppm): 182.50 (C-1); 170.91 (C-7); 130.45 (C-9); 136.81 (C-11); 136.17 (C-13); 163.94 (C-12); 120.77 (C-8); 128.87 (C-10); 55.39 (C-6); 26.72 (C-2); 43.14 (C-5); 30.43 (C-4,4′); 29.15 (C-3,3′); 38.01 (C-14)carbon are assigned with numbers as presented in Numbering Scheme 3.

### 2.3. Synthesis of organotin(IV) carboxylates

For synthesis of organotin(IV) carboxylates **(1–6)**, a two neck round bottom flask fitted with a condenser was charged with

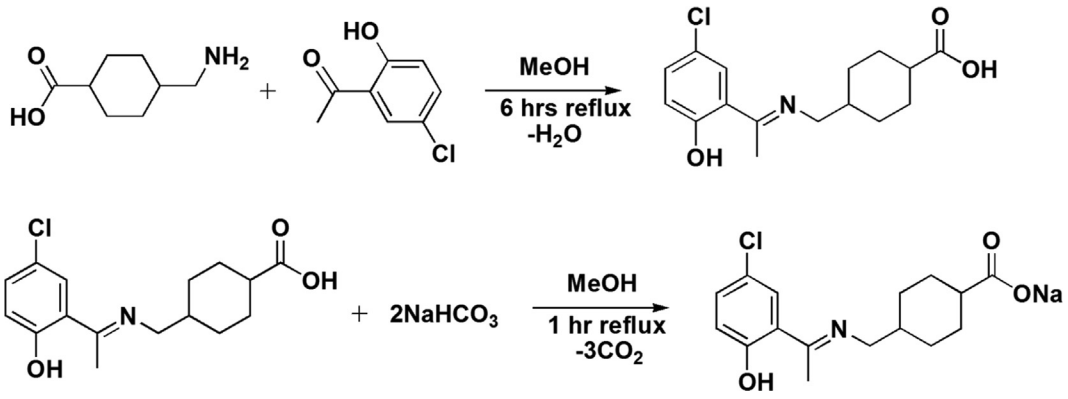


**Scheme 1.** Synthesis of sodium salt of ligand **(NaL)**.

sodium salt of ligand (0.5 g, 1.5 mmol) and respective organotin (IV) precursor$(CH_3)_2SnCl_2$ (0.16 g, 0.75 mmol)/$(C_4H_9)_2SnCl_2$ (0.22 g, 0.75 mmol)/$(CH_3)_3SnCl$ (0.3 g, 1.5 mmol), $(C_4H_9)_3SnCl$ (0.49 g, 1.5 mmol)/$(C_6H_5)_3SnCl$ (0.58, 1.5 mmol) in 100 mL dry toluene. The reaction mixture was refluxed for 8 h till a visible change occurred. The reaction mixture was then kept overnight, and sodium chloride formed was removed by filtration. The n-dioctyltin(IV) oxide(0.29 g, 0.8 mmol) was reacted with free ligand (0.5 g, 1.6 mmol)in toluene and water formed was removed by Dean Stark apparatus (Choudhary, Bhatti, & Ali, 2012). The reaction mixture was refluxed for 8 h, and solvent was removed under reduced pressure. The obtained product was re-crystallized from chloroform n-hexane (1:4) mixture (Nadeem Muhammad et al., 2020). the reaction is summarized in Scheme 2.

*2.3.1. Dibutyltin(IV)bis[4-((5-chloro-2-hydroxyphenyl) ethylideneamino)methyl)cyclohexane carboxylate]; (1)*

Yield: 68%, m.p. 205–207 °C: anal. calc. for $C_{40}H_{56}Cl_2N_2O_6Sn$: C, 56.49 (55.84); H, 6.64 (5.33); N, 3.29 (3.54); IR (4000–400 $cm^{-1}$): 1632 $\upsilon(COO)_{sym}$;1477 $\upsilon(COO)_{asym}$; 155 $\Delta\upsilon$; 1586 $\upsilon$(C = N); 3373 $\upsilon(OH)_{phenolic}$; 453 $\upsilon$(Sn-O); 567 $\upsilon$(Sn-C): $^1$H NMR ($CDCl_3$-d) $\delta$ (ppm): 7.20 (d, *J* = 8.8 Hz, 1H, phenyl), 7.45 (s, 1H, phenyl), 6.84 (d, *J* = 8.9 Hz, 1H, phenyl), 3.42 (d, *J* = 5.6 Hz, 2H, $-NCH_2$), 2.3 (s, 3H, $CH_3$), 2.46–2.50 (m, 1H, cyclohexyl), 2.07–2.10 (m, *J* = 13.2, 7.7, 6.1, 4.9 Hz, 4H, cyclohexyl), 1.44–1.46 (m, *J* = 13.2, 4H, cyclohexyl), 1.43 (t, 4H, α-H), 1.12–1.12 (m, 4H, β,γ-H), 0.93 (t, 6.72, 6H, δ-H). $^{13}$C NMR ($CDCl_3$-d) δ (ppm): 192.26 (C-1), 168.20 (C-7), 156.80 (C-9), 148.70 (C-11), 118.69 (C-13), 127.23 (C-12), 123.08 (C-8), 110 (C-10), 57.98 (C-2), 41.45 (C-5), 34.82 (C-4,4′),28.73 (C-3,3′), 30.67 (C-γ), 26.13 (C- β),25.69 (C-α), 14.88 (C-14), 14.16 (C-δ).

*2.3.2. Dimethyltin(IV)bis[4-((5-chloro-2-hydroxyphenyl) ethylideneamino)methyl)cyclohexane carboxylate]; (2)*

Yield: 73%, m.p. 182–184 °C: 766.34: anal. calc. for $C_{34}H_{44}Cl_2N_2O_6Sn$: C, 53.29 (52.88): H, 5.79 (5.63): N, 3.66 (3.56): IR (4000–400 $cm^{-1}$): 1652 $\upsilon(COO)_{sym}$;1466 $\upsilon(COO)_{asym}$; 186 $\Delta\upsilon$; 1594 $\upsilon$(C = N); 3387 $\upsilon(OH)_{phenolic}$; 466 $\upsilon$(Sn-O); 570 $\upsilon$(Sn-C): $^1$H NMR ($CDCl_3$-d) δ (ppm): 7.20 (d, 8.1 Hz, 1H, phenyl); 6.85 (d, *J* = 8.8 Hz, 1H, phenyl);3.41 (d, *J* = 5.5 Hz, 2H, $-NCH_2$); 2.33 (s, 3H, $CH_3$); 1.92–1.95 (m, 1H, cyclohexyl); 1.38–1.41 (m, 4H, cyclohexyl); 1.26–1.30 (m, 4H, cyclohexyl)1.09–1.11 (m, 1H, cyclohexyl); 0.93 (s, 6H, αH): $^{13}$C NMR ($CDCl_3$-d) δ (ppm): 172.26 (C-1); 161.6 (C-7); 159.5 (C-9); 132.69 (C-11); 129.08 (C-12); 122.50 (C-8); 116.16 (C-10); 57.95 (C-6); 42.45 (C-2); 37.25 (C-5); 36.82

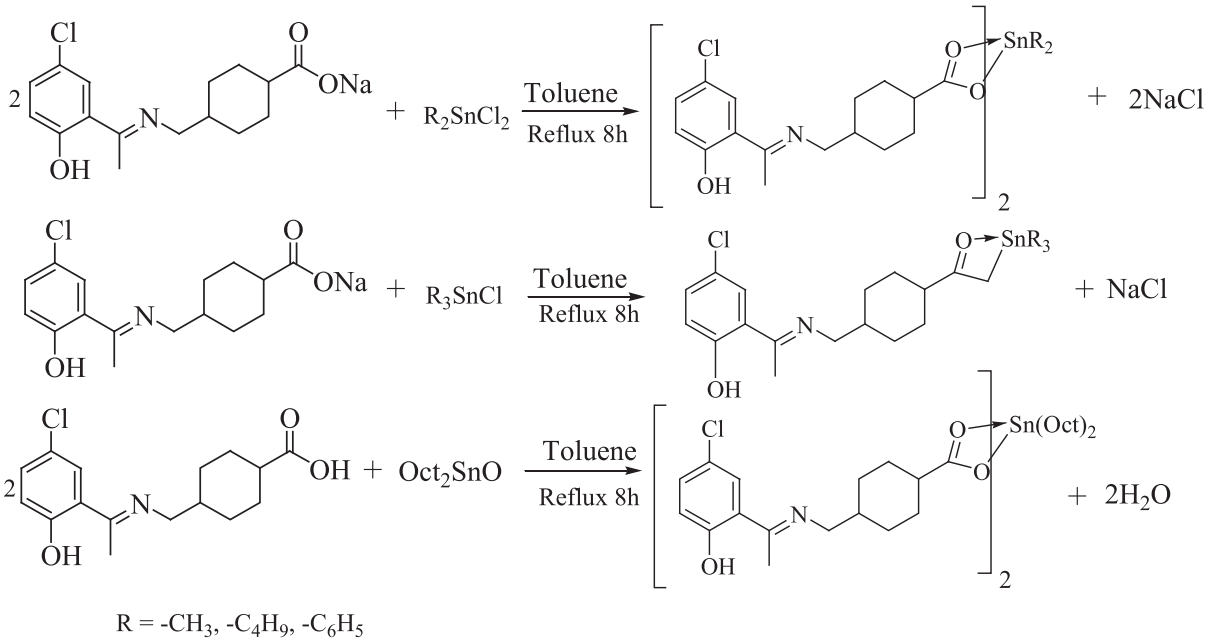


**Scheme 2.** Synthesis of organotin(IV) carboxylates.

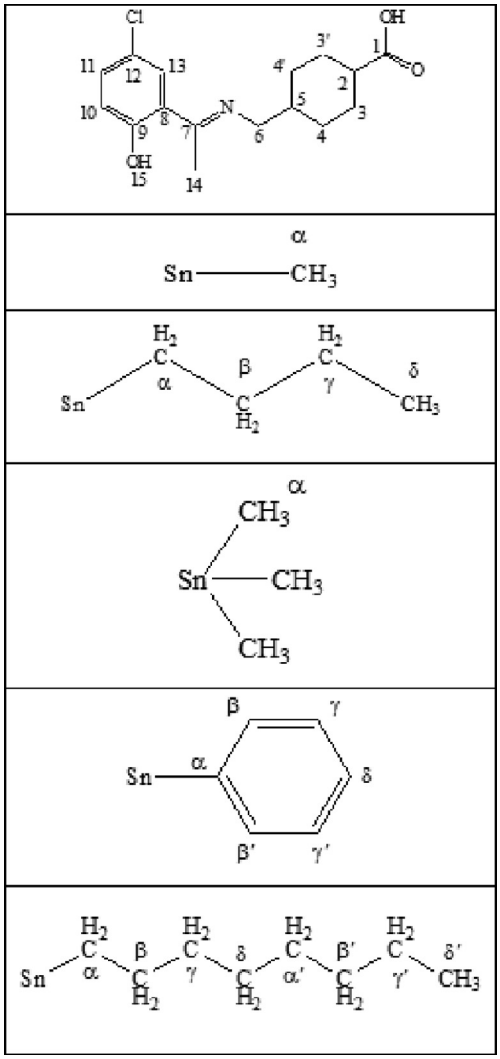

**Scheme 3.** $^{13}C$ & $^{1}H$ numbering scheme.

(C-4,4′); 28.67 (C-3,3′);18.48 (C-α); 17.86 (C-14) (Numbering Scheme 3).

*2.3.3. Trimethyltin(IV)bis[4-((5-chloro-2-hydroxyphenyl) ethylideneamino)methylcyclohexane carboxylate]; (3)*

Yield: 71%, m.p. 215–217 °C: 472.59: anal. calc. for $C_{19}H_{28}ClNO_3Sn$: C, 48.29 (47.93); H, 5.97 (5.77); N, 2.96 (2.45): IR (4000–400 $cm^{-1}$): 1652 $\upsilon(COO)_{sym}$;1474 $\upsilon(COO)_{asym}$; 178 $\Delta\upsilon$; 1584 υ(C = N); 3422 $\upsilon(OH)_{phenolic}$; 453 υ(Sn-O); 561 υ(Sn-C): $^{1}H$ NMR ($CDCl_3$-d) δ (ppm): 7.45 (s, 1H, phenyl), 7.22 (d, *J* = 8.9 Hz, 1H, phenyl), 6.85 (d, *J* = 8.8 Hz, 1H, phenyl), 3.42 (d, *J* = 6.5 Hz, 2H, $-NCH_2$), 2.32 (s, 3H, $CH_3$), 2.06–2.09 (m, 1H, cyclohexyl), 1.43–1.46 (m, 4H, cyclohexyl), 1.27–1.30 (m, 4H, cyclohexyl), 1.12–1.15 (m, 1H, cyclohexyl), 0.53 (s, 9H, α-H).: $^{13}C$ NMR ($CDCl_3$-d) δ (ppm): 183.81 (C-1), 173.30 (C-7), 166.44 (C-12), 135.02 (C-11), 129.79 (C-13), 123.37 (C-8), 121.78 (C-10), 57.16 (C-6), 46.16 (C-2), 40.50 (C-5), 32.96 (C-4,4′), 31.61 (C-3,3′), 16.76 (C-α), 2.44 (C-14).

*2.3.4. Tributyltin(IV)bis[4-((5-chloro-2-hydroxyphenyl) ethylideneamino)methyl)cyclohexane carboxylate]; (4)*

Yield: 76%, m.p. 232–234 °C: 598.84: anal. calc. for $C_{28}H_{46}ClNO_3Sn$: C, 56.16 (56.01); H, 7.74 (7.62); N, 2.34 (2.21): IR (4000–400 $cm^{-1}$): 1647 $\upsilon(COO)_{sym}$;1467 $\upsilon(COO)_{asym}$; 180 $\Delta\upsilon$; 1543 υ(C = N); 3337 $\upsilon(OH)_{phenolic}$; 432 υ(Sn-O); 554 υ(Sn-C): $^{1}H$ NMR ($CDCl_3$-d), δ (ppm): 7.63 (s,1H, phenyl), 7.26 (d, *J* = 6.3 Hz,1H, phenyl), 7.74 (d, *J* = 6.3 Hz,1H, phenyl), 3.43 (d, *J* = 6.5 Hz, 2H, $-NCH_2$), 2.37 (s, 3H, $CH_3$), 1.87–1.90 (m, 1H, cyclohexyl), 1.84 – 1.76 (m, 4H, cyclohexyl), 1.31–1.34 (m, 4H, cyclohexyl), 1.26 – 1.29 (m, 1H, αH), 1.30–1.33 (m, *J* = 7.2 Hz, 4H, γH), 1.06–1.09 (m, 4H, βH), 0.86 (t, *J* = 7.3 Hz, 6H, δH): $^{13}C$ NMR ($CDCl_3$-d), δ (ppm): 183.44 (C-1), 172.77 (C-7), 165.15 (C-9), 132.57 (C-11), 128.38 (C-12), 121.29 (C-13), 119.47 (C-8), 119.33 (C-10), 54.63 (C-2), 44.97 (C-5), 39.59 (C-4,4′), 28.23 (C-γ), 26.81 (C-α), 29.71 (C- β), 14.80 (C-δ), 14.13 (C-14).

*2.3.5. Triphenyltin(IV)bis[4-((5-chloro-2-hydroxyphenyl) ethylideneamino)methyl)cyclohexane carboxylate]; (5)*

Yield: 78%, m.p. 245–248 °C: 658.8: anal. calc. for $C_{34}H_{34}ClNO_3Sn$: C, 61.99 (61.54); H, 5.20 (5.10); N, 2.13 (2.01): IR (4000–400 $cm^{-1}$): 1625 $\upsilon(COO)_{sym}$;1440 $\upsilon(COO)_{asym}$; 185 $\Delta\upsilon$; 1532 υ (C = N); 3336 $\upsilon(OH)_{phenolic}$; 434 υ(Sn-O); 545 υ(Sn-C): $^{1}H$ NMR ($CDCl_3$-d) δ (ppm): 7.69 (m, 1H, phenyl), 7.47 (d, 1H, δH) 7.45 (s, 1H, phenyl), 7.43 (d, 1H, βH, β′H), 7.25 – 7.14 (m, 1H, γH, γH), 6.83 (d, *J* = 8.9 Hz, 1H, phenyl), 3.40 (d, *J* = 5.7 Hz, 2H, $-NCH_2$), 2.62 (s, 3H, $CH_3$), 1.91–1.94 (m, 1H, cyclohexyl), 1.51–1.54 (m, 4H, cyclohexyl), 1.26–1.29 (m,4H, cyclohexyl), 1.11–1.14 (m, 1H, cyclohexyl).: $^{13}C$ NMR ($CDCl_3$-d) δ (ppm): 182.50 (C-1), 170.89 (C-7), 163.90 (C-9), 160.91 (C-10), 137.53 (C-12), 137.26 (C-9), 130.36 (C-α), 128.66 (C-β), 127.0 (C-γ), 119.74 (C-δ), 120.12 (C-11), 129.16 (C-8),55.41 (C-6), 43.14(C-2), 38.01(C-5), 30.43 (C-4,4′), 26.72 (C-3,3′), 14.35 (C-14).

*2.3.6. Dioctyltin(IV)bis[4-((5-chloro-2-hydroxyphenyl) ethylideneamino)methyl)cyclohexane carboxylate]; (6)*

Yield: 73%, m.p. 192–194 °C: anal. calc. for $C_{48}H_{72}C_{l2}N_2O_6Sn$: C, 59.88 (59.56); H, 7.54 (7.34); N, 2.91(2.76): IR (4000–400 $cm^{-1}$): 1655 $\upsilon(COO)_{sym}$;1482 $\upsilon(COO)_{asym}$; 173 $\Delta\upsilon$; 1563 υ(C = N); 3364 $\upsilon(OH)_{phenolic}$; 473 υ(Sn-O); 581 υ(Sn-C): $^{1}H$ NMR ($CDCl_3$-d) δ (ppm): 8.16 (s, 1H, OH), 6.98 (d, *J* = 6.6 Hz, 1H, phenyl), 7.02 (s, 1H, phenyl), 6.95 (d, 1H, phenyl), 3.47 (d, *J* = 6.6 Hz, 2H, $-NCH_2$), 2.32–2.36 (m, 1H, cyclohexyl), 2.28 (s, 3H, $-CH_3$), 1.59–1.61 (m, 4H, cyclohexyl), 2.06 (t, *J* = 14.1 Hz, 4H, α′H), 1.94–1.97 (m, 4H, cyclohexyl), 1.30–1.33 (m, 4H, β-β′H), 1.251.30 (bs, γ--γ′H), 1.21 – 1.23 (m, 6H, δH), 0.90 (t, *J* = 6.2 Hz, 2H, αH).: $^{13}C$ NMR ($CDCl_3$-d) δ (ppm): δ 173.30 (C-1), 166.44 (C-7), 135.03 (C-11), 129.80 (C-12), 123.20 (C-8), 121.79 (C-10), 57.89 (C-2), 46.16 (C-5), 40.51 (C-4,4′), 25.12 (C-3,3′), 32.97 (C-γ), 31.87 (C-β), 31.62 (C-α) 30.50 (C-γ), 27.97 (C-β′), 26.97 (C-β), 18.97 (C-δ′), 16.76 (C-δ).

*2.4. Biological applications*

*2.4.1. Antileishmanial assay*

Antileishmanial activity of the synthesized compounds was evaluated *in vitro* against the promastigote form of *leishmaniatropica* using XTT (2, 3-bis-(2-methoxy-4-nitro-5-dulfophenyl)–2H-tetrazolium-5-carboxanilide) based assay as a marker of cell viability (Meyre-Silva et al., 2013). Stock solution (5 mg/mL) of XTT was prepared in phosphate buffer solution and stored in dark at 4 °C. RPMI-1640, fetal bovine serum (FBS), potassium chloride (KCl), sodium bicarbonate ($NaHCO_3$), phosphate buffer saline (PBS), antibiotic (Penicillin/Streptomycin) and distilled water were used in preparation of culture medium. For anti-leishmaniasis, each well of the 96-well plate was charged 100 μL culture media and $2.5 \times 10^4$ cells/mL were seeded into each well. The seedling density was counted during log phase using a Neubauer chamber. The promastigotes were allowed to enter to their log phase until the count reach from 5 to 6 million cells per mL. Three different concentrations (1.25 μg/mL, 2.5 μg/mL, and 5 μg/mL) of each compound were added to respective wells in 96-well plate. Amphotericin B

was used as a reference drug and DMSO as negative control. The 96- well plate was incubated for 72 h at 25 ± 1 °C. After incubation 10 μL of XTT was added to each well and was again incubated for 3 h at 25 °C. 40 μL of DMSO was then added into each well of the plate as stopping solution and relative optical density (OD) the plate was recorded at 450 nm using an ELISA plate reader. The number of viable cells is correlated by the absorbance of formazan produced by the mitochondrial dehydrogenase of active cells (C. Williams et al., 2003). All the experiments were performed in triplicate and the Percent inhibitions of the compounds were calculated using the following formula:

$$\text{Percent Inhibition} = \frac{\text{mean OD of Sample} - \text{mean OD of Blank}}{\text{mean OD of positive control} - \text{mean OD of Blank}} \times 100$$

*2.4.2. DNA interaction study*

DNA interaction study was carried out by UV–visible spectroscopy. SS-DNA (20 mg) was dissolved in water by overnight stirring. 20 mM PBS was used to check the percent purity of DNA by a ratio of UV absorbance at 260 and 280 nm. The final concentration of the SS-DNA solution was determined by using molar extinction coefficient (6,600 $M^{-1}cm^{-1}$) and was found to be 180 mM. A series of DNA solution (5 μM, 10 μM, 15 μM, 20 μM and 25 μM) were treated with test compounds (3 mM, 3 mL). The solutions were incubated for 5 min and then subjected to UV–visible absorption. Absorption spectra were recorded using quartz cuvettes in the range 600–200 nm (Sirajuddin, Ali, & Badshah, 2013).

*2.4.3. Antioxidant activity*

DPPH standard protocol was applied for antioxidant study (Yabalak, Emire, Adıgüzel, Könen Adıgüzel, & Gizir, 2020). DPPH solution (160 μM) was prepared in ethanol. To a series of test compounds (25 μM, 50 μM, 75 μM, 100 μM and 125 μM) DPPH solution (3 mL, 160 μM) was added. UV–visible absorption of the solutions at 517 nm was recorded using quartz cuvettes after being incubated for 2 min(Adeyemi et al., 2019).

*2.4.4. Cytotoxicity*

Brine shrimp's lethality bioassay was used to evaluate the cytotoxicity of synthesized compounds. Briefly, a vessel was filled with sterile simulated sea water. The sea water was prepared by adding sea salt (38 g/L) and pH was adjusted to 8.5, using NaOH solution. Brine shrimp's eggs were added to this sea water at room temperature. The eggs were hatched into brine shrimps after two days continuous aeration. Thirty active nauplii were collected in a vial containing yeast suspension and 4.5 mL brine solution. a series of three vials containing 4.5 mL brine solution and yeast suspension were provided with 0.5 mL test compounds solution with different concentrations (5, 50 and 100 μg/mL). The experiment was conducted in triplicate. Etoppside was used as standard reference drug. $LD_{50}$ was determined by using Finney's probit analysis.

*2.4.5. Antifungal activity*

Antifungal activity of the compounds was done by using standard agar tube dilution method. Five fungal strains *F. Solani, C. Albicans, T. Longifusus, A. Flavis* and *M. Canis* were tested. Miconazole and amphotericin were used as standard drugs. Growth media sabouraud dextrose was prepared by mixing glucose agar (45%), sabouraud (32.5 g), and agar (20 g) in 500 mL distilled water at 90 °C. 4 mL media was added into respective capped tubes and autoclaved for 15 min at 121 °C. 100 μg/mL of each test compounds was added to respective tube at 50 °C and the media was then solidified at room temperature. The tubes were then provided with 4 mm inoculums derived from a seven day old fungal culture. The tubes were then incubated at 25 °C for 8 days. Each fungal strain growth was measured with linear growth in mm and growth inhibition was calculated with reference to respective standard (Nural, Gemili, Yabalak, De Coen, & Ulger, 2018).

*2.4.6. Antibacterial activity*

Antibacterial activity of the synthesized compounds was assisted by agar well diffusion essay. Five bacterial strains including *E. Coli, B. Subtillus, S. Aureus P. Aeruginosa* and *S. Typhi* were checked. Briefly, petri plates were provided with nutrient agar growth media at 50C and solidified at room temperature. Growth media nutrient agar was prepared by standard procedure. Wells were bored in the media with the help of 6 mm sterile cork borer. Bacterial strains of about five hours old bacterial inoculums were spread on the surface of media using sterile cotton swab. Test compounds (100 μg/mL), standard reference (Imipenem) and negative control (DMSO) was provided into their respective wells. The prepared plates were incubated at 37C for 20 h. The antibacterial activity was determined by measuring zone of inhibition in millimeter. Growth inhibition was calculated with reference to standard drug (Nural et al., 2018).

## 3. Results and discussions

### 3.1. FT-IR

The FT-IR spectra of free ligand, its di and tri-organotin(IV) carboxylates were recorded in the range 4000–400 $cm^{-1}$. Characteristic frequencies of $\upsilon(COO)_{asym,}$ $\upsilon(COO)_{sym,}$ υ(OH), υ(C = O) and υ (C = N) were identified in the prepared compounds (Xue et al., 2022). The data together with bands assigned to υ(Sn-O) and υ (Sn-C) is presented in the experimental section. The presence of characteristics bands, around 3400 $cm^{-1}$ and 1686 $cm^{-1}$ can be assigned to the stretching vibrations of OH and C = N functional groups (Sarıarslan, Karaca, Şahin, & Pekmez, 2020). Furthermore these bands also confirm the formation of ligand **(**Fig. S1, Supplementary materials**)**(Dahmani et al., 2021). Comparison of IR spectra of ligand and orgnaotin(IV) complexes reveal the appearance of new bands around 535–567 $cm^{-1}$ and 440–450 $cm^{-1}$ assignable to υ(Sn-C) and υ(Sn-O) stretching vibrations (Nadeem Muhammad et al., 2018). The spectra are shown in Figures S2-S7 (Supplementary materials). The bonding mode of the ligand was determined by Δυ, {$\upsilon_{asym}$(COO) - $\upsilon_{sym}$(COO) value which was in the range 150–180 $cm^{-1}$signified that the ligand is a chelated bidentate (**1, 3, 6, 7**) and bridging bidentate (**2, 5**) as presented in experimental section(Amir, Khan, Shah, & Butler, 2014; Wang et al., 2017). The Δυ value in the rang 150–250 $cm^{-1}$ presents bridging and less than 150 $cm^{-1}$ indicates a chelate structure (Niaz Muhammad, Ali, Meetsma, & Shaheen, 2009).

### 3.2. NMR spectroscopy

Multinuclear magnetic resonance spectroscopy is one of the most extensively used techniques for characterization of organotin(IV) complexes. This technique is used to determine the parameters like spin multiplicity, peak intensity, pattern, integration and coupling constant $^2J(^{119}Sn,^1H)$, $^1J(^{119}Sn,^{13}C)$ (Arshad, Bhatti, Farooqi, Saleem, & Mirza, 2016). These parameters afford information about the geometry of organotin(IV) complexes (Debnath et al., 2020).

*3.2.1. $^1$HNMR*

NMR spectra of the prepared ligand and its organotin(IV) carboxylates were recorded in deuterated chloroform using TMS as internal standard and the data is given in experimental section.

The $^{1}H$ and $^{13}C$ NMR spectra of ligand and complexes **(1–6)** are shown in supplementary data (Fig. S8-S20, Supplementary materials). In the $^{1}H$ NMR spectrum of ligand, resonance signals for protons of cyclohexyl OH, phenyl, methyl and methylene groups with characteristic multiplicity and integration confirmed the formation of ligand (Aman, Matela, Sharma, & Chaudhary, 2015). However, in spectra of complexes (**1**–**6**), in addition to ligand characteristic signal, the appearance of respective alkyl/aryl group resonance signals attached to tin atom indicted the formation of complexes. The protons attached to cyclohexyl appeared as multiples in the range of at 1.00–2.32 ppm and methylene group resonate as doublet around 3.44 ppm (Fig S8-S20, Supplementary materials) (Hussain et al., 2014). Whereas the $^{1}H$ resonances of methyl group attached to N of the azomethine appears as singlet around 2.35 ppm. The protons of the aromatic part of the ligand appeared as two set of dupletsin the range of 6.74–7.37 ppm. The protons of alkyl/aryl groups attached to tin showed signals as expected. Coupling constant $^{2}J(^{119}Sn, ^{1}H)$ and Lockhart equation was used to determine the coordination around Sn atom. The calculated values for $^{2}J(^{119}Sn, ^{1}H)$ of compounds **2** and **3** were 83 and 79 Hz, agreeing with C-Sn-C angle of 132.87 and 130.15°, respectively, demonstrating five coordination around tin (Table 1) (Rabiee, Safarkhani, & Amini, 2019).

### 3.2.2. $^{13}C$ NMR

The $^{13}C$ NMR spectra displayed the carbon resonance of the ligand and coordinated Sn-R.The exact number of carbon resonance at their characteristics chemical shift values validated the formation of ligand and complexes (**1–6**). The carboxylate carbons resonance of free ligand at 182.50 ppm is shifted downfield to 192.26**(1)**, 183.81 **(3)**, 183.44 **(4)**and 185.2**(6)**ppm in complexes verifying COO-Sn coordination. These chemical shifts are consistent with that reported for butanoic acid (Tariq et al., 2014){Tariq, 2014 #1;Tariq, 2014 #1}. Similarly, the shifting of carboxylic carbon resonance to downfield compared to free ligand strongly recommending coordination via carboxylate group. No extra resonance signals were found in $^{13}C$ NMR and thus suggesting the purity of compounds. The cyclohexyl carbons resonances are observed in the range 26–43 ppm. The other resonance lines in the spectra fall in the three regions, i.e., 14–26 ppm for aliphatic, 110–138 ppm for carbons of phenyl group and 172–192 ppm for carbonyl carbon of carboxyl group (Akintayo, Munzeiwa, Jonnalagadda, & Omondi, 2021).

### 3.2.3. XRD analysis

Powder XRD diffraction pattern of the compounds (**1–6**) were recorded by Oxford X-calibur Gemini diffractometer**.** The spectra exposed sharp peaks with prominent diffraction intensities and low background. Expert high score plus software was used to determine the indexing of powder diffraction pattern and searching space group of the crystal specimens (Fig. 1) (Akremi & Noubigh, 2019). The structural features and properties obtained are demonstrated in Fig.1 (Supplementary materials). The indexed 10 prominent diffraction lines of ligand demonstrated lattice parameter of orthorhombic crystal system with primitive bravais and P 21 am space group. Similarly the complexes 1 and 2 indexed lattice parameters fitted to orthorhombic crystal system with C face centered and primitive bravais (Masciocchi, Sironi, Chardon-Noblat, & Deronzier, 2002). Scherrer equation was used to calculate the crystallite size D of complexes **1, 2** and **3**and found to be 142 nm, 76 nm and 70 nm respectively (Xue, Kamali, Yu, Appels, & Dewil, 2023).

$$D = \frac{k\lambda}{\beta\cos\theta}$$

Where D is the crystal size in the form of powder, *K* shape factor with value of unity, $\lambda$ is wavelength of X-ray, $\beta$ is FWHM and $\theta$ is Bragg angle.

PXRD data shows that all the prominent diffraction pattern of prepared compounds can be readily indexed by a set of lattice parameter. The relative deviations between experimental and calculated are about 1.12%, 0.45% and 0.36% for compounds **1, 2** and **3** correspondently, which could suggest that all the prepared compounds are single phase(Su et al., 2022).

### 3.3. Biological activity

#### 3.3.1. Antileishmanial activity

*In vitro* antileishmanial activity of the prepared was done using XTT standard protocol against promestigotes form *leishmaniatropica* (Ozlem-Caliskan, Ertabaklar, Bilgin, & Ertug, 2021). The examined compounds produced a significant reduction in viable promestigotes. The complexes showed high antileishmanial activity compared to the free ligand suggesting the charge distribution and compatibility of the compounds structure to cell membrane enzyme trypanothione synthetase. All the test concentrations showed significant antileishmanial activity (Fig. 2). The $IC_{50}$ of the compounds and standard is shown in Table 2. The compounds **1, 2** and **5** were most potent against promestigotes form of *leishmaniatropica* and exhibited $IC_{50}$ value 1.22 ± 0.014, 1.17 ± 0.007 and 1. 22 ± 0.021 μg/mL as compared to the positive standard amphotericin B which exhibited 0.71 ± 0.05 μg/mL value. Compounds **3** and **6** also showed remarkable potency with $IC_{50}$ 1.68 ± 0.014 and 1.94 ± 0.03 respectively against *leishmaniatropica* as demonstrated in Table 2. The ligand and compound **4** were found inactive. The antileishmanial activity may be due to the interference with the functioning of *leihmania* mithocondria (Ozlem-Caliskan et al., 2021). This investigation demonstrated the potential use of the prepared organotin(IV) carboxylate as a source of novel agents for the treatment of leishmaniasis.

#### 3.3.2. DNA interaction

The DNA-compounds interaction was examined by UV–Visible spectroscopy. The synthesized compounds (**1–6**) were interacted with different concentrations of DNA and UV–Visible spectra were taken (Fig. 3).The compounds showed two bands around 250 nm and 350 nm which are probably due to aromatic $\pi$ - $\pi^*$ transition and 300–380 nm due to n - $\pi^*$ transition of CO or NC groups. As the DNA was interacted with increasing concentration, hypochromic effect, and red shift of about 5 nm in the bands were observed.

**Table 1**
Coupling constant and C-Sn-C angles of complexes.

| Compound Code | $^{2}J(^{119}Sn, ^{1}H)$ | $^{1}J(^{119}Sn, ^{13}C)$ | Angle (o) | |
|---|---|---|---|---|
| | | | $\theta(^{2}J)$ | $\theta(^{1}J)$ |
| 1 | ———— | ———— | ———— | ———— |
| 2 | 83 | ———— | (132.8°) | ———— |
| 3 | 79 | ———— | (130.1°) | ———— |

Key: Code 1 = Dibutyletin(IV), Code 2 = Dimethyltin(IV), and Code 3 = Trimethyltin(IV) derivative of ligand (HL).

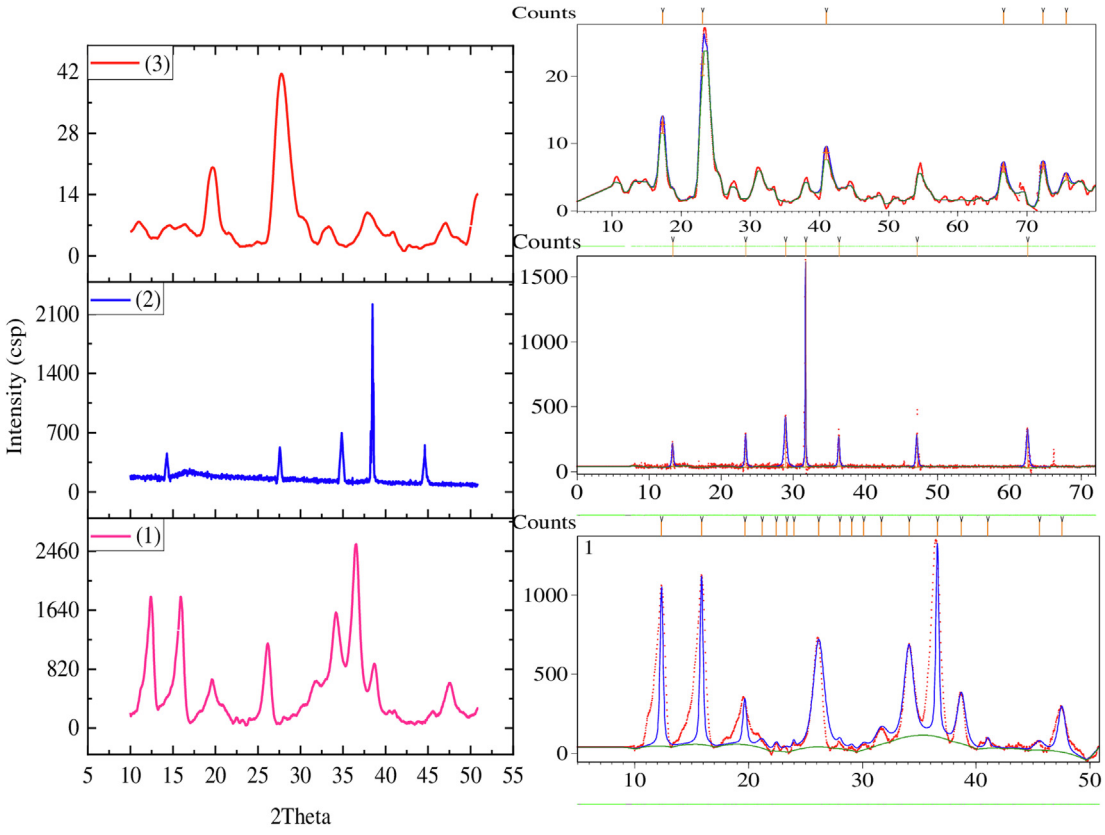


**Fig. 1.** Powder XRD pattern of complexes **1–3** and peaks indexation using X-pert high score plus software 10[3].

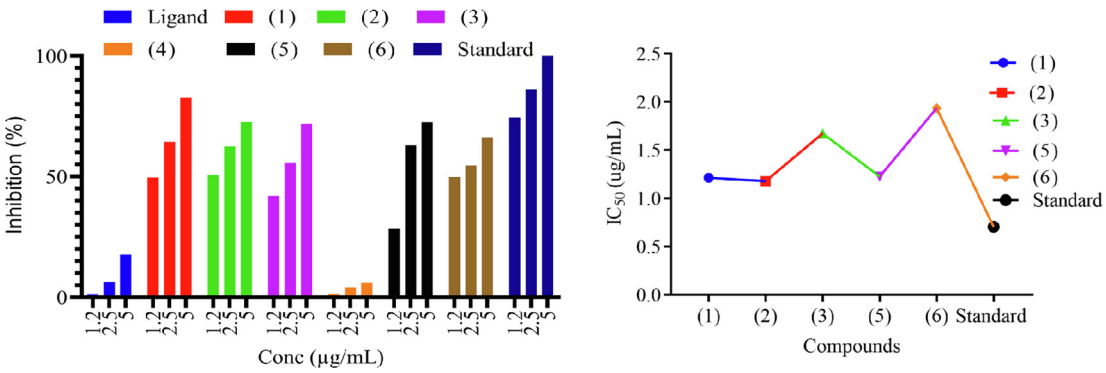


**Fig. 2.** Antileishmanial activity; Percentage inhibition and $IC_{50}$ of selected compounds.

The band shift of molecules after interacted with DNA could be evidence of binding mode of DNA with small molecules (Casini et al., 2001). In case of intercalative mode of binding, hypochromism effect coupled with red shift for the characteristic's peaks will be observed due to strong stacking between DNA base pairs and chromophores of the compounds. Thus, the interaction between small molecules and DNA could be non-covalent intercalative binding. During intercalation of the base pairs of DNA, the $\pi^*$ orbital of the ligand could couple with $\pi$ orbital of the DNA base pairs, thus resulting in bathochromic effect due to lowering $\pi$ -$\pi^*$ transition energy. Similarly, the coupling of partially filled electrons with $\pi$ orbital lowers the transition likelihood and hence result hypochromism. The hypochromic effect may be observed due to $\pi$ - $\pi^*$ (stacking interaction) in intercalative binding mode and bathochromic effect is observed when DNA duplex is stabilized (Aydinoglu et al., 2016). In case of compounds (**2,3** and**5**) the DNA-compounds complex showed stability as revealed from red shift after 12 and 24 h. The intrinsic binding constant of com-

**Table 2**
Antileishmanial activity of 4-((5-chloro-2-hydroxyphenyl)ethylideneamino)methyl)-cyclohexanecarboxylic acid (HL) and itsorganotin(IV) complexes.

| Sample Code | $IC_{50}$(μg/mL) ± SD |
|---|---|
| HL | – |
| **1** | 1.22 ± 0.01 |
| **2** | 1.17 ± 0.01 |
| **3** | 1.68 ± 0.01 |
| **4** | – |
| **5** | 1.22 ± 0.02 |
| **6** | 1.94 ± 0.03 |
| Amphotericin B | 0.71 ± 0.01 |

Key: Code **1** = $Bu_2SnL$, Code **2** = $Me_2SnL$, Code **3** = $Me_3SnL$, Code **4** = $Bu_3SnL$], Code **5** = $Ph_3SnL$, and Code **6** = *n*-$Oct_2SnL$.

pounds with DNA, based on variation in band shift, was calculated by using Benesi-Hildebrands equation.

$$\frac{A_0}{A - A_0} = \frac{\varepsilon_G}{\varepsilon_{H-G} - \varepsilon_G} + \frac{\varepsilon_G}{\varepsilon_{H-G} - \varepsilon_G} X \frac{1}{K[\mathrm{DNA}]}$$

Where *K* is binding/association constant, $A_0$ and A are the absorbance of compound and DNA-compound complex, respectively. $\varepsilon_G$is the absorption coefficient of compound and $\varepsilon_{H\text{-}G}$is the absorption coefficient of DNA-compound complex. The binding constants *K* were calculated from intercept to slop ratio of $A_0/(A\text{-}A_0)$ *vs* 1/[DNA]. The intrinsic binding constants of compounds (**2, 3, 4** and **5**) are determined to 2.7 × $10^3$, 1.7 × $10^3$, 1.1 × $10^2$and 6.2 × $10^3$ respectively as demonstrated in Table 3 and Fig. 3. The compounds (**2, 3, 4** and **5**) showed significant binding constant whereas the ligand and compound (**1** and**6**) were inactive. Gibbs free energy was calculated from equation: ΔG = -RT lnK.

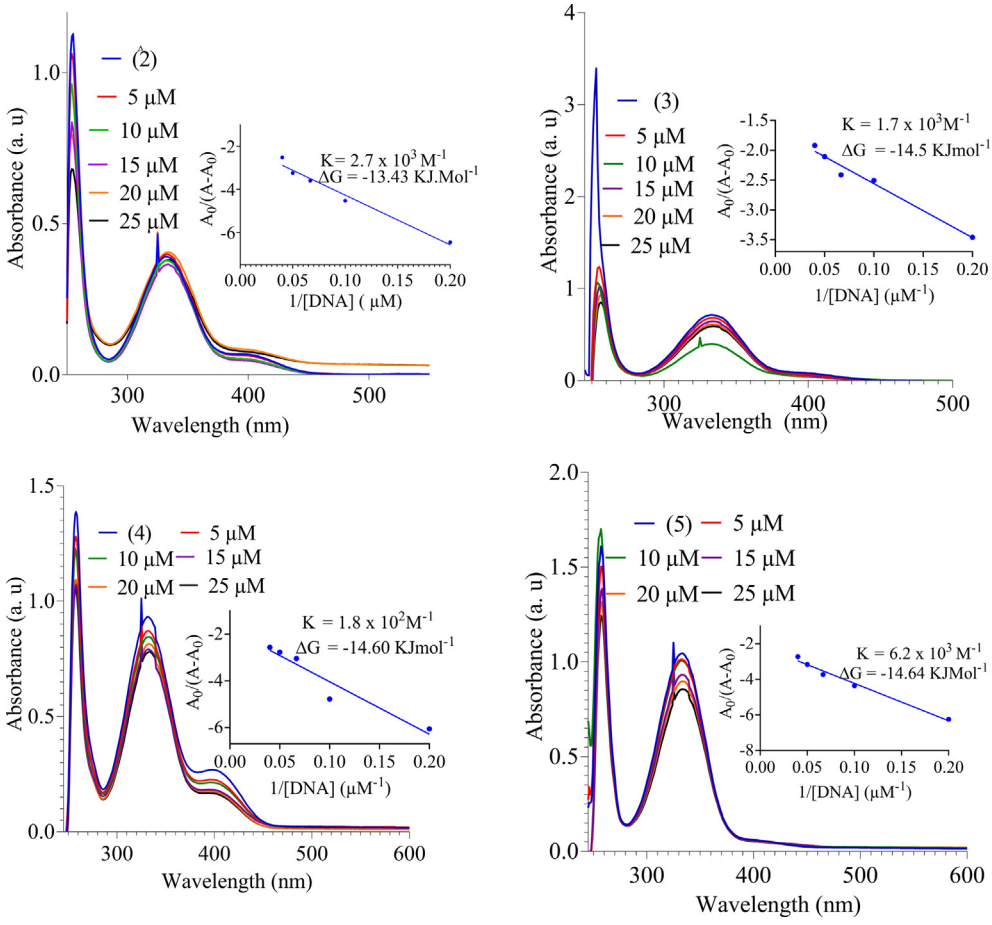


**Fig. 3.** UV–Vis spectra of DNA binding study and DNA binding constant.

**Table 3**
DNA binding constant and Gibbs free energy of organotin(IV) compounds.

| Compound-DNA | *K* ($M^{-1}$) | -ΔG ($KJmol^{-1}$) |
|---|---|---|
| 2-DNA | 2.7 × $10^3$ | 13.43 |
| 3-DNA | 1.7 × $10^3$ | 14.5 |
| 4-DNA | 1.8 × $10^2$ | 14.60 |
| 5-DNA | 6.2 × $10^3$ | 14.64 |

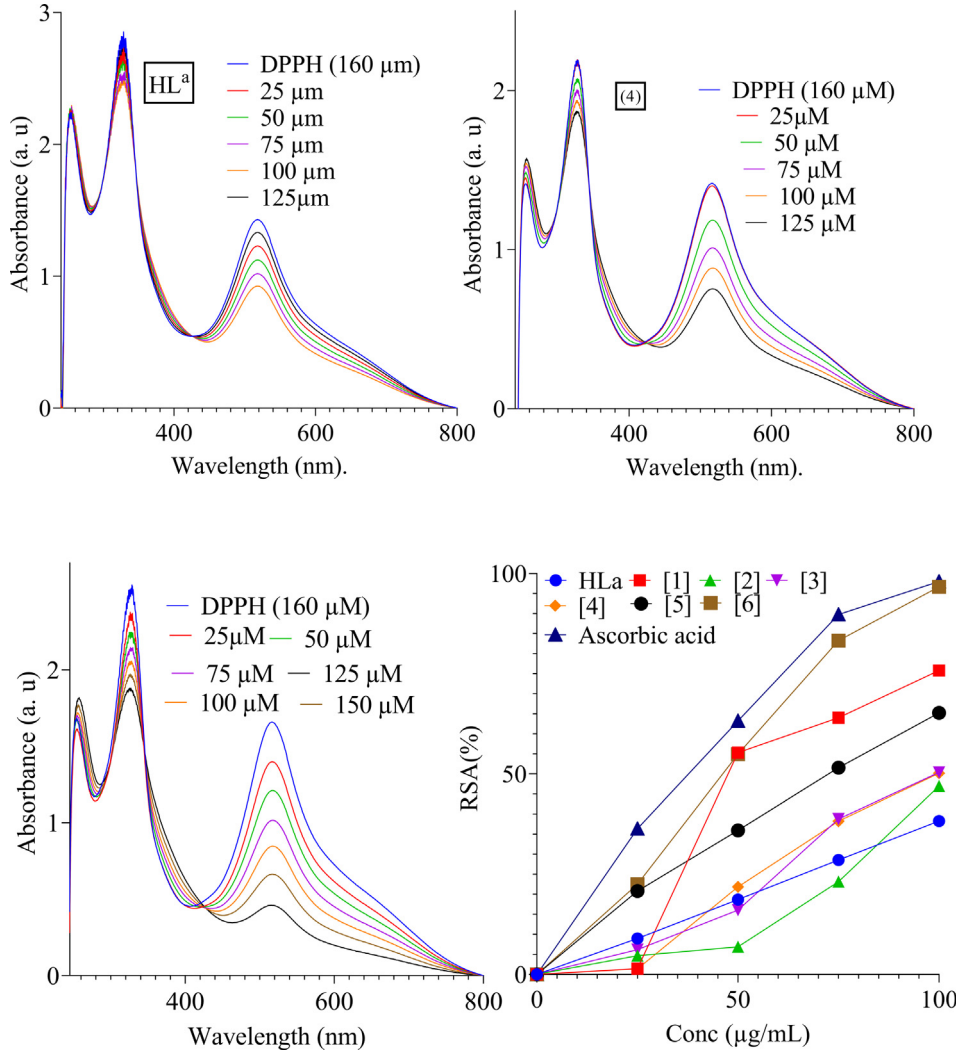


**Fig. 4.** Antioxidant activity of **HL, (3), (4), (5)** and % RSA.

**Table 4**
Antioxidant activity of ligand (**HL**) and its complexes (**1**–**6**).

| Compounds | $IC_{50}$ (MM) |
|---|---|
| HL | ––––– |
| **1** | 76.92 ± 0.93 |
| **2** | 56.31 ± 1.13 |
| **3** | 92.58 ± 1.53 |
| **4** | 112.59 ± 1.03 |
| **5** | 42.10 ± 1.43 |
| **6** | 116.33 ± 0.83 |
| Ascorbic acid | 37.35 ± 0.36 |

Key: Code **1** = $Bu_2SnL$, Code **2** = $Me_2$-SnL, Code **3** = $Me_3SnL$, Code **4** = $Bu_3$-SnL], Code **5** = $Ph_3SnL$, and Code **6** = *n*-$Oct_2SnL$.

R is gas constant (8.314 $JK^{-1}.mol^{-1}$), T is temperature (298 K). The values of ΔG and *K* are given in the inset graph (Fig. 3). The order of DNA-compound interaction is as **5**>**2**>**3**>**4.**The compounds might interact with nitrogenous base of the DNA and restrain cell growth by interfering the transcription and replication of DNA. The DNA interaction study revealed that these compounds may be used as anticancer drugs.

*3.3.3. Antioxidant activity*

Health pathologies such as diabetes, heart diseases, are all contributed by oxidative damage. The antioxidants agents can slow down or prevent oxidative damage to our body by converting the free radicals to stabile components. DPPH standard protocol was used to investigate the antioxidant activity of free ligand and compounds (**1**–**6**) (Sari, Qudus, & Hadi, 2020). The compounds showed significant percentage antioxidant activity range from 96% to 59% compared to free ligand (46%) (Fig. 4). The low $IC_{50}$ values (76.92, 56.31 and 42. 10 MM) of Compounds (**1, 2** and **5**) suggested significant antioxidant activity (Table 4 and Fig. 4). In the complexes, the phenolic group gives hydrogen radical and results the initiation of radical chain and they act as antioxidant agents. Similarly, the electronegative halogen substituent and conjugated system also served good antioxidant. Overall, the complexes showed comparable antioxidant activity reported in the previous work (Yabalak et al., 2020).

*3.3.4. Cytotoxicity*

The ability of organotin(IV) complexes to interact with cell membrane, protein and DNA make them cytotoxic. The toxicity of the synthesized compound against Brine shrimps was tested. All the tested complexes revealed significant toxicity except ligand which showed moderate toxic effect (Table.5 and Fig. 5). Highest

**Table 5**
Toxicity and $LD_{50}$ values of ligand and complexes (1–6).

| Comp. No | Dose μg/mL | No. of killed shrimps from 30/dilution | $LD_{50}$ (μg/mL) |
|---|---|---|---|
| HL | 5 | 02 | 14.22 |
| | 50 | 05 | |
| | 100 | 10 | |
| 1 | 5 | 08 | 8.65 |
| | 50 | 14 | |
| | 100 | 20 | |
| 2 | 5 | 11 | 6.26 |
| | 50 | 17 | |
| | 100 | 24 | |
| 3 | 5 | 12 | 6.79 |
| | 50 | 22 | |
| | 100 | 27 | |
| 4 | 5 | 5 | 14.56 |
| | 50 | 10 | |
| | 100 | 20 | |
| 5 | 5 | 13 | 5.67 |
| | 50 | 19 | |
| | 100 | 28 | |
| 6 | 5 | 10 | 9.98 |
| | 50 | 17 | |
| | 100 | 26 | |
| Standard | 5 | 13 | 5.80 |
| | 50 | 20 | |
| | 100 | 28 | |

Key: Code **1** = $Bu_2SnL$, Code **2** = $Me_2SnL$, Code **3** = $Me_3SnL$, Code **4** = $Bu_3SnL$], Code **5** = $Ph_3SnL$, and Code **6** = *n*-$Oct_2SnL$.

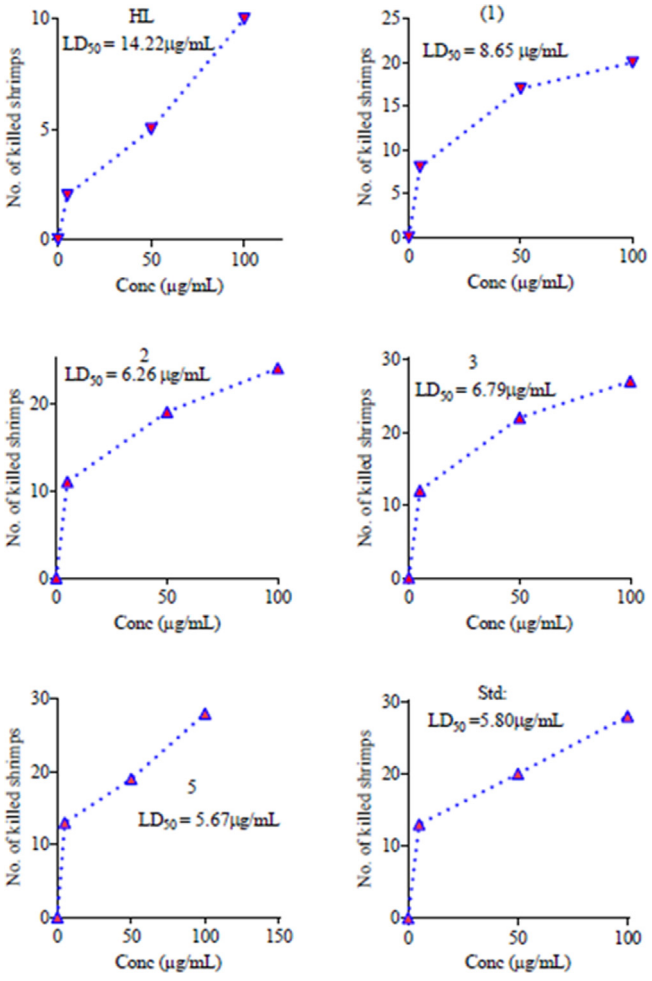


**Fig. 5.** *In vitro* cytotoxicity of Organotin(IV) complexes with $LD_{50}$ against *Brine Shrimps* 30/dilution.

toxicity was observed for complex **3** (27 killed Brine shrimps 30/dilution) and **5** (28 killed Brine shrimps 30/dilution) which is almost similar to the standard drug (27 killed Brine shrimps 30/dilution). The lowest toxicity was found for ligand and complex **4** with $LD_{50}$ values of 14.22 μg/mL and 14.56 μg/mL. The $LD_{50}$ values of complexes **2** (6.26 μg/mL), **3** (6.79 μg/mL) and **5** (5.67 μg/mL) indicated comparable toxicity to standard drug (5.80 μg/mL). The high cytotoxicity of complexes (**3** and **5**) may be due to the presence of phenyl group. In addition to bioactive pharmacophore and bulky cyclohexyl, the phenyl group facilitates π-π interaction between biomolecules and complexes. The complexes showed potent cytotoxicity lower $LD_{50}$ value comparable to the previously reported work (Yabalak et al., 2017; Nural et al., 2018).

### 3.3.5. Antifungal

Based on the provided data, different strains of fungi were tested for their susceptibility to various drugs, and the results are presented in terms of percentage inhibition and minimum inhibitory concentration (MIC) values (Table. 6 and Fig. 6). All the organotin(IV) derivatives of ligand revealed significant activity against tested fungal strains. Highest activity was found for complex 5 with % inhibition in the range 25–74%, where the complex was most effective against *F. solani* and *M. canis* with 72% and 74% inhibition respectively. Similarly, the complex (4) and (6) also showed significant activity, however the complexes revealed highest effectiveness against *A. flayis* and *F. solani* with growth inhibition of 55% and 68% respectively. Furthermore, the complexes (**1, 2** and **3**) were found most active against *F. solani, A. falyis* and *F. solani* respectively. All the complexes showed highest antifungal activity against *F. solani*. The ligand was found active against *A. falyis* and *F. solani* and inactive for other tested fungal strains. The lowest MIC (32 μg/mL and 43 μg/mL) was found for complex (5) and (6) respectively (Table. 6). The high antifungal activity of complexes may be due to the coordination and polarity of tin with oxygen of the ligand. The complexes (**1, 2** and **3)** showed high activity which may be due to the increase lipophilicity and permeability across the cell membrane (Hussain et al., 2015).

**Table 6**
Anti-fungal data of ligand and organotin(IV) complexes.

| Fungus strains (ATCC) | (%) Inhibition | | | | | | | Standard drugs | MIC (μg/mL) |
|---|---|---|---|---|---|---|---|---|---|
| | HL | (1) | (2) | (3) | (4) | (5) | (6) | | |
| *C. albicans* (2192) | 12 | 32 | 41 | 37 | 43 | 64 | 53 | Amphotericine B | 76 |
| *T. longifusus* (22397) | 05 | 28 | 38 | 30 | 47 | 52 | 48 | Miconazole | 63 |
| *A. flavis* (1030) | 47 | 38 | 53 | 43 | 55 | 68 | 50 | Miconazole | 32 |
| *F. solani* (11712) | 53 | 58 | 52 | 50 | 54 | 72 | 68 | Miconazole | 51 |
| *M. canis* (9865) | 18 | 37 | 48 | 38 | 42 | 74 | 58 | Miconazole | 43 |

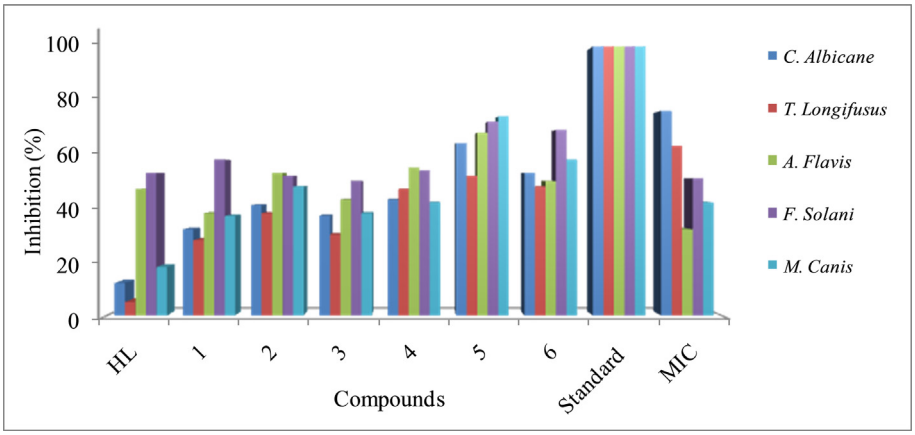


**Fig. 6.** Comparative antifungal %inhibition of ligand and complexes with standard.

**Table 7**
Antibacterial data of ligand and organotin(IV) complexes.

| Bacterial strains | HL | C1 | C2 | C3 | C4 | C5 | C6 | Standard |
|---|---|---|---|---|---|---|---|---|
| *B. subtilis* | 15 | 18 | 23 | 21 | 12 | 28 | 25 | 32 |
| *E. coli* | 5 | 14 | 16 | 15 | 18 | 27 | 20 | 30 |
| *S. aureus* | 10 | 15 | 18 | 13 | 11 | 23 | 19 | 25 |
| *S. typhi* | 16 | 17 | 15 | 14 | 13 | 19 | 17 | 22 |
| *P. aeruginosa* | 18 | 20 | 19 | 23 | 21 | 23 | 20 | 25 |

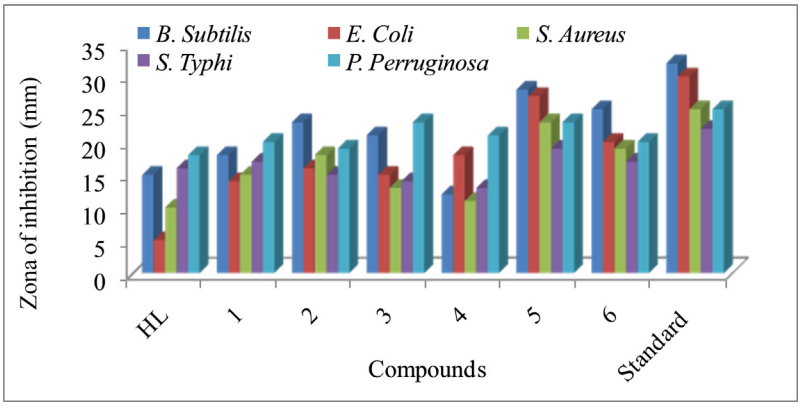


**Fig. 7.** Antibacterial activity of ligand and its organotin(IV) complexes.

*3.3.6. Antibacterial*

The synthesized ligand and its organotin(IV) complexes revealed antibacterial activity against the targeted bacterial strains (Table. 7 and Fig. 7). The ligand was found active against *P. aeruginosa* (18/25 mm) and *S. typhi* (16/22 mm), inactive against *E. coli* (5/30 mm) and moderately active against *B. subtillus* (15/32 mm) and *S. aureus* (10/25 mm). All the complexes showed significant activity against the tested bacterial strains compared to lignad. The highest activity was observed for complexes (**5 & 6**) against all tested bacterial strains among test complexes. The complexes (**1, 2 and 3**) showed moderate activity against *B. subtillus*, *E. coli*, *S. aureus* and *S. typhi*. The data revealed that all the complexes

showed highest activity against *S. typhi* and *P. aerruginosa*. The antibacterial potential of these complexes revealed that the substituted bioactive pharmacophore containing complexes are of biological properties. The activity of these complexes can be attributed to the bulky cyclohexyl and active pharmacophore substituent that is good electron donating groups, enhancing the lipophilic property of complexes by strengthening ligand metal bond. The antibacterial result is corroborated to previously report tin complexes.

## 4. Conclusions

In conclusion, this study encompassed a comprehensive characterization of six novel organotin(IV) carboxylates derived from 4-((1-(5-chloro-2-hydroxyphenyl)ethylideneamino)methyl)cyclohexanecarboxylic acid. The application of elemental analysis, FT-IR, NMR ($^{1}$H, $^{13}$C), and PXRD techniques offered a thorough understanding of the structural attributes of these compounds. Notably, the coordination geometry around organotin(IV) was established as five-coordinate, with ligand binding occurring in a bidentate manner, as evidenced by NMR and FTIR analyses. Furthermore, our investigation into the antileishmanial activity of these complexes unveiled significant potency in complexes 1, 2, and 5, highlighting their potential as potent antileishmanial agents. The evaluation of DNA binding revealed a compelling binding affinity in complexes 2 to 5, while complexes 1 and 6 displayed inactivity in this context. The order of DNA-compound interaction strength was determined as 5>2>3>4. Notably, complexes 1, 2, and 5 exhibited substantial antioxidant activity, underscoring their potential utility in oxidative stress modulation. These findings collectively underscore the promising biological and chemical attributes of the synthesized organotin(IV) carboxylates, presenting avenues for further exploration in therapeutic and medicinal applications.

## CRediT authorship contribution statement

**Shah Hussain:** Conceptualization,Methodology,Formal analysis, Data curation,Resources,Validation,Visualization,Writing - original draft.**Shaukat Shujah:** Supervision,Formal analysis,Conceptualization,Methodology,Validation,Visualization,Writing - original draft. **AbdulRehman:** Critical Review and Editing. **Syed Tasleem Hussain:** Formal analysis,Data curation,Methodology,Resources,Validation,Visualization,Writing - review & editing.**Mubbashir Hussain:** Supervision,Formal analysis,Methodology,Resources,Validation,Visualization,Writing - original draft,Writing - review & editing. **Iffat Naz:** Critical Review and Editing. **Aiyeshah Alhodaib:** Critical Review and Editing.

## Declaration of Competing Interest

The authors declare that they have no known competing financial interests or personal relationships that could have appeared to influence the work reported in this paper.

## Acknowledgments

The researchers would like to thank the Deanship of Scientific Research, Qassim University for funding the publication of this project.

## Ethics approval

Not applicable as no human or animals were involved in this study.

## Funding Source

The Deanship of Scientific Research, Qassim University for funding the publication of this project.

## Appendix A. Supplementary material

Supplementary data to this article can be found online at https://doi.org/10.1016/j.arabjc.2023.105306.

## References

Abbas, S.M., Ali, S., Hussain, S.T., Shahzadi, S., 2013. structural diversity in organotin (IV) dithiocarboxylates and carboxylates. J. Coord. Chem. 66 (13), 2217–2234.
Adeyemi, J.O., Onwudiwe, D.C., Ekennia, A.C., Anokwuru, C.P., Nundkumar, N., Singh, M., Hosten, E.C., 2019. Synthesis, characterization and biological activities of organotin (IV) diallyldithiocarbamate complexes. Inorg. Chim. Acta 485, 64–72.
Akintayo, D.C., Munzeiwa, W.A., Jonnalagadda, S.B., Omondi, B., 2021. Ring-opening polymerization of cyclic esters by 3-and 4-pyridinyl Schiff base Zn (II) and Cu (II) paddlewheel complexes: kinetic, mechanistic and tacticity studies. Arab. J. Chem. 14, (10) 103313.
Akremi, A., Noubigh, A., 2019. New organotin (IV) chlorides derived from N-(2-hydroxyphenyl) aryloxy sulfamates. Synthesis, characterization and DSC investigation. J. Chem. Sci. 131 (2), 1–8.
Alotaibi, S. H., & Momen, A. A. (2019). Anticancer drugs' deoxyribonucleic acid (DNA) interactions. In *Biophysical Chemistry-Advance Applications*: IntechOpen.
Aman, R., Matela, G., Sharma, C., Chaudhary, S., 2015. Biologically active diorganotin (IV) complexes of N-(2-hydroxy-3-isopropyl-6-methyl benzyl) glycine. Arab. J. Chem. 8 (5), 698–705.
Amir, M.K., Khan, S., Shah, A., Butler, I.S., 2014. Anticancer activity of organotin (IV) carboxylates. Inorg. Chim. Acta 423, 14–25.
Arshad, N., Bhatti, M.H., Farooqi, S.I., Saleem, S., Mirza, B., 2016. Synthesis, photochemical and electrochemical studies on triphenyltin (IV) derivative of (Z)-4-(4-cyanophenylamino)-4-oxobut-2-enoic acid for its binding with DNA: biological interpretation. Arab. J. Chem. 9 (3), 451–462.
Aydinoglu, S., Biver, T., Figuccia, S., Fiore, T., Montanaro, S., Pellerito, C., 2016. Studies on DNA interaction of organotin (IV) complexes of meso-tetra (4-sulfonatophenyl) porphine that show cellular activity. J. Inorg. Biochem. 163, 311–317.
Casini, A., Messori, L., Orioli, P., Gielen, M., Kemmer, M., Willem, R., 2001. Interactions of two cytotoxic organotin (IV) compounds with calf thymus DNA. J. Inorg. Biochem. 85 (4), 297–300.
Chen, K., Zhao, B.S., He, C., 2016. Nucleic acid modifications in regulation of gene expression. Cell Chem. Biol. 23 (1), 74–85.
Choudhary, M.A., Bhatti, M.H., Ali, S., 2012. Synthesis, structural elucidation and biological activities of organotin (IV) derivatives of (E)-3-(4-methoxyphenyl)-2-(4-chlorophenyl)-2-propenoic acid. J. Iran. Chem. Soc. 9 (1), 35–45.
Dahmani, M., Harit, T., Et-Touhami, A., Yahyi, A., Eddike, D., Tillard, M., Benabbes, R., 2021. Two novel macrocyclic organotin (IV) carboxylates based on bipyrazoledicarboxylic acid derivatives: Syntheses, crystal structures and antifungal activities. J. Organomet. Chem. 948, 121913.
Debnath, P., Singh, K.S., Devi, T.S., Singh, S.S., Butcher, R.J., Sieroń, L., Maniukiewicz, W., 2020. Synthesis, characterization, crystal structures and anti-diabetic activity of organotin (IV) complexes with 2-(4-hydroxynaphthylazo)-benzoic acid. Inorg. Chim. Acta 510, 119736.
Goto, H., Lindoso, J., 2004. Immunity and immunosuppression in experimental visceral leishmaniasis. Braz. J. Med. Biol. Res. 37 (4), 615–623.
Gradoni, L., 2018. A brief introduction to leishmaniasis epidemiology. In: The Leishmaniases: Old Neglected Tropical Diseases. Springer, pp. 1–13.
Hadi, A.G., Jawad, K., Ahmed, D.S., Yousif, E., 2019. Synthesis and biological activities of organotin (IV) carboxylates: a review. Systemat. Rev. Pharm. 10 (1), 26–31.
Hussain, S., Ali, S., Shahzadi, S., Tahir, M.N., Shahid, M., 2015. Synthesis, characterization, biological activities, crystal structure and DNA binding of organotin (IV) 5-chlorosalicylates. J. Coord. Chem. 68 (14), 2369–2387.
Hussain, S., Ali, S., Shahzadi, S., Sharma, S. K., Qanungo, K., & Shahid, M. (2014). Synthesis, characterization, semiempirical and biological activities of organotin (IV) carboxylates with 4-piperidinecarboxylic acid. *Bioinorganic Chemistry and Applications, 2014*.
Kumar, A., Pandey, S.C., Samant, M., 2020. A spotlight on the diagnostic methods of a fatal disease Visceral Leishmaniasis. Parasite Immunol. 42 (10), e12727.
Lipoldová, M., Demant, P., 2006. Genetic susceptibility to infectious disease: lessons from mouse models of leishmaniasis. Nat. Rev. Genet. 7 (4), 294–305.
Maltezou, H.C., 2008. Visceral leishmaniasis: advances in treatment. Recent Pat. Antiinfect. Drug Discov. 3 (3), 192–198.
Masciocchi, N., Sironi, A., Chardon-Noblat, S., Deronzier, A., 2002. X-ray powder diffraction study of organometallic polymers:[Ru (L)(CO) 2] n (L= 2, 2 '-bipyridine or 1, 10-phenanthroline). Organometallics 21 (19), 4009–4012.
Meyre-Silva, C., Niero, R., Bolda Mariano, L. N., Gomes do Nascimento, F., Vicente Farias, I., Gazoni, V. F., . . . Salamanca, E. (2013). Evaluation of antileishmanial activity of selected Brazilian plants and identification of the active principles. *Evidence-Based Complementary and Alternative Medicine, 2013*.

Mohammed, A.S.A., Tian, W., Zhang, Y., Peng, P., Wang, F., Li, T., 2020. Leishmania lipophosphoglycan components: a potent target for synthetic neoglycoproteins as a vaccine candidate for leishmaniasis. Carbohydr. Polym. 237, 116120.

mondiale de la Santé, O., & Organization, W. H. (2016). Leishmaniasis in high-burden countries: an epidemiological update based on data reported in 2014. *Weekly Epidemiological Record= Relevé épidémiologique hebdomadaire, 91*(22), 286-296.

Muhammad, N., Ali, S., Meetsma, A., Shaheen, F., 2009. Organotin (IV) 4-methoxyphenylethanoates: synthesis, spectroscopic characterization, X-ray structures and in vitro anticancer activity against human prostate cell lines (PC-3). Inorg. Chim. Acta 362 (8), 2842–2848.

Muhammad, N., Rahman, A., Younis, M.A., Subhani, Q., Shehzad, K., Cui, H., Zhu, Y., 2018. Porous SnO2 nanoparticles based ion chromatographic determination of non-fluorescent antibiotic (chloramphenicol) in complex samples. Sci. Rep. 8 (1), 12327.

Muhammad, N., Zhang, Y., Subhani, Q., Intisar, A., Mingli, Y., Cui, H., Zhu, Y., 2020. Comparative steam distillation based digestion of complex inorganic copper concentrates samples followed by ion chromatographic determination of halogens. Microchem. J. 158, 105176.

Muhammad, N., Zia-ul-Haq, M., Ali, A., Naeem, S., Intisar, A., Han, D., Rahman, A., 2021. Ion chromatography coupled with fluorescence/UV detector: A comprehensive review of its applications in pesticides and pharmaceutical drug analysis. Arab. J. Chem. 14, (3) 102972.

Nural, Y., Gemili, M., Yabalak, E., De Coen, L., & Ulger, M. (2018). Green synthesis of highly functionalized octahydropyrrolo [3, 4-c] pyrrole derivatives using subcritical water, and their anti (myco) bacterial and antifungal activity. *Arkivoc*(5), 51-64.

Olías-Molero, A.I., de la Fuente, C., Cuquerella, M., Torrado, J.J., Alunda, J.M., 2021. Antileishmanial drug discovery and development: Time to reset the model? Microorganisms 9 (12), 2500.

Ozlem-Caliskan, S., Ertabaklar, H., Bilgin, M. D., & Ertug, S. (2021). Evaluation of photodynamic therapy against Leishmania tropica promastigotes using different photosensitizers. *Photodermatology, photoimmunology & photomedicine*.

Prieto-Bermejo, R., Romo-González, M., Pérez-Fernández, A., Ijurko, C., Hernández-Hernández, Á., 2018. Reactive oxygen species in haematopoiesis: leukaemic cells take a walk on the wild side. J. Exp. Clin. Cancer Res. 37 (1), 1–18.

Rabiee, N., Safarkhani, M., Amini, M.M., 2019. Investigating the structural chemistry of organotin (IV) compounds: recent advances. Rev. Inorg. Chem. 39 (1), 13–45.

Sari, W., Qudus, H.I., Hadi, S., 2020. The chemical reactivity study of organotin (IV) 4-aminobenzoates using cyclic voltammetry and antioxidant activity test by the DPPH method. Rev. Chim. 71 (10), 28–37.

Sarıarslan, H., Karaca, E., Şahin, M., Pekmez, N.Ö., 2020. Electrochemical synthesis and corrosion protection of poly (3-aminophenylboronic acid-co-pyrrole) on mild steel. RSC Adv. 10 (63), 38548–38560.

Sirajuddin, M., Ali, S., Badshah, A., 2013. Drug–DNA interactions and their study by UV–Visible, fluorescence spectroscopies and cyclic voltametry. J. Photochem. Photobiol. B Biol. 124, 1–19.

Su, H.-Q., Zhang, R.-F., Guo, Q., Wang, J., Li, Q.-L., Du, X.-M., Ma, C.-L., 2022. Five organotin complexes derived from hydroxycinnamic acid ligands: Synthesis, structure, in vitro cytostatic activity and binding interaction with BSA. J. Mol. Struct. 1247, 131290.

Tariq, M., Ali, S., Muhammad, N., Shah, N.A., Sirajuddin, M., Tahir, M.N., Khan, M.R., 2014. Biological screening, DNA interaction studies, and catalytic activity of organotin (IV) 2-(4-ethylbenzylidene) butanoic acid derivatives: synthesis, spectroscopic characterization, and X-ray structure. J. Coord. Chem. 67 (2), 323–340.

Tariq, M., Khan, R., Hussain, A., Batool, A., Rasool, F., Yar, M., Ali, S., 2021. Synthesis, characterization, antimicrobial, cytotoxic, DNA-interaction, molecular docking and DFT studies of novel di-and tri-organotin (IV) carboxylates using 3-(3-nitrophenyl) 2-methylpropenoic acid. J. Coord. Chem. 74 (14), 2407–2426.

Tiwari, N., Kumar, A., Singh, A.K., Bajpai, S., Agrahari, A.K., Kishore, D., Singh, R.K., 2019. Leishmaniasis control: Limitations of current drugs and prospects of natural products. In: Discovery and Development of Therapeutics from Natural Products Against Neglected Tropical Diseases. Elsevier, pp. 293–350.

Wang, H., Hu, L., Du, W., Tian, X., Zhang, Q., Hu, Z., Tian, Y., 2017. Two-photon active organotin (IV) carboxylate complexes for visualization of anticancer action. ACS Biomater. Sci. Eng. 3 (5), 836–842.

Williams, C., Espinosa, O.A., Montenegro, H., Cubilla, L., Capson, T.L., Ortega-Barrıa, E., Romero, L.I., 2003. Hydrosoluble formazan XTT: its application to natural products drug discovery for Leishmania. J. Microbiol. Methods 55 (3), 813–816.

Williams, D.B.G., Lawton, M., 2010. Drying of organic solvents: quantitative evaluation of the efficiency of several desiccants. J. Org. Chem. 75 (24), 8351–8354.

Xue, Y., Guo, Y., Zhang, X., Kamali, M., Aminabhavi, T.M., Appels, L., Dewil, R., 2022. Efficient adsorptive removal of ciprofloxacin and carbamazepine using modified pinewood biochar–A kinetic, mechanistic study. Chem. Eng. J. 450, 137896.

Xue, Y., Kamali, M., Yu, X., Appels, L., Dewil, R., 2023. Novel CuO/Cu2 (V2O7)/V2O5 composite membrane as an efficient catalyst for the activation of persulfate toward ciprofloxacin degradation. Chem. Eng. J. 455, 140201.

Yabalak, E., Adiguzel, S.K., Adiguzel, A.O., Ergene, R.S., Tuncer, M., Gizir, A.M., 2017. Application of response surface methodology for the optimization of oxacillin degradation by subcritical water oxidation using H2O2: genotoxicity and antimicrobial activity analysis of treated samples. Desalin. Water Treat. 81, 186–198.

Yabalak, E., Emire, Z., Adıgüzel, A.O., Könen Adıgüzel, S., Gizir, A.M., 2020. Wide-scale evaluation of Origanum munzurense Kit Tan & Sorger using different extraction techniques: Antioxidant capacity, chemical compounds, trace element content, total phenolic content, antibacterial activity and genotoxic effect. Flavour Fragr. J. 35 (4), 394–410.

Zafar, R., Shahid, K., Wilson, L.D., Fahid, M., Sartaj, M., Waseem, W., Ullah, S., 2021. Organotin (IV) complexes with sulphonyl hydrazide moiety. Design, synthesis, characterization, docking studies, cytotoxic and anti-leishmanial activity. J. Biomol. Struct. Dyn., 1–11